SAND2014-4653C

Uncertainty Quantification for Multiscale Thermal Transport Simulations

Leslie M. Phinney, William W. Erikson, and Jeremy B. Lechman
Engineering Sciences Center, Sandia National Laboratories, Albuquerque, New Mexico, 87185, USA

Two of the more recent developments in thermal transport simulations are the incorporation of multiscale models and requirements for verification, validation, and uncertainty quantification to provide actionable simulation results. The aleatoric uncertainty is investigated for a two component mixture containing a high thermal conductivity and a low thermal conductivity material. The microstructure is varied from a coarse size of 1/8 the domain length to a fine scale of 1/256 the domain length and for volume fractions of high thermal conductivity material from 0 to 1. The uncertainty in the temperatures is greatest near the percolation threshold of around 0.4 and for the coarsest microstructures. Statistical representations of the aleatoric uncertainty for heterogeneous materials are necessary and need to be passed between scales in multiscale simulations of thermal transport.

Nomenclature

d	=	dimensionality of geometry
f	=	volume fraction
L	=	domain length
T	=	temperature
A	=	subscript designating material A
B	=	subscript designating material B
mix	=	subscript designating material mixture
λ	=	thermal conductivity

I. Introduction

Multiscale computational approaches are increasingly employed for heat transfer and fluid dynamics simulations since increases in computing power have enabled ever greater fidelity in models and simulations.[1-3] Many systems and processes involve geometries and structures which span from macroscale down to microscale including transport in heterogeneous media and microdevices. The use of multiscale modeling techniques requires verification and validation (V&V) and uncertainty quantification (UQ) methods applicable to these simulations in order to provide actionable data for decisions.[4] Verification ensures that the simulation mathematics and code are correctly computing the solution to the model equations while validation compares the simulation results to the physical problem being modeled. UQ calculates the statistical range by which a simulation result differs from the true value.[5-7] To provide an illustrative example, we focus on thermal transport in heterogeneous media and UQ implications in such a material.

Thermal transport in heterogeneous or disordered media requires knowledge of the material microstructure, especially at short length scales.[8] An example of a heterogeneous media is a material containing two constituents, one with a high thermal conductivity and a second with a lower thermal conductivity. Many models have been developed for the effective thermal conductivity in such a material as well as bounds on the value.[9-14] For uncertainty quantification, the variability in the material properties are needed in addition to the mean thermal property. For a layer containing two materials, effective thermal conductivities and their variation are predicted for a given microstructure revealing the stochastic nature and inherent uncertainty present.[8,14] The data needed to determine and propagate uncertainty are discussed. This paper advances the development of multiscale transport modeling by examining the application of UQ to porous media.

II. Uncertainty Quantification

Computational multiscale modeling has been applied to problems in material science such as fracture in brittle materials[15] and nanocrystalline plasticity.[16] A recent review of uncertainty quantification in multiscale materials simulations summarizes the types of uncertainty, representation of uncertainty, uncertainty propagation, and use of sensitivity analysis.[15] Two types of uncertainty are aleatory (inherent randomness) and epistemic (lack of knowledge). Aleatory uncertainty can be described statistically and more data can help to better represent the variability in the material properties. Epistemic uncertainty is due to bias, incorrect models, or missing physics in the model and cannot be represented statistically.[5,6,15] A major challenge to applying UQ to multiscale models is the propagation of uncertainties between scales.[17] Most multiscale models can be classified as information-passing or concurrent. Information-passing multiscale methods use computational schemes targeted for a specific scales. The calculations at finer scales obtain values such as accommodation coefficients or effective material properties that are used in larger scale simulations. Concurrent multiscale models are used for problems in which it is necessary to resolve multiple scales to capture the phenomena of interest such as fracture. In these schemes, information is passed between subdomains represented by different models resolving the necessary scales. For both information-passing and concurrent methods, UQ requires that not only the relevant quantities themselves but also the statistics associated with those quantities be preserved and passed between scales.[17] Sensitivity analysis can be employed to highlight the variables to which the transport processes are most sensitive and future efforts should be focused to reduce uncertainty. We examine the aleatoric uncertainty associated with material variability in a heterogeneous composite in the next section.

III. Thermal Transport in Porous Media

We utilize a steady state thermal conduction (Fourier's law) model to illustrate UQ for heterogeneous media. The model is a two-dimensional steady state calculation on a square domain (5.12 cm on a side) in which the west side (x=0) is held at T_1=100 and the east side (x=L) is held at T_2=0. The south (y=0) and north (y=L) sides are treated as periodic boundary conditions, such that $T_{north} = T_{south}$ at every value of x. The domain was meshed using uniform linear quadrahedral finite elements of size 0.01 cm such that the overall domain is 512x512 elements.

Two different materials were used in the model: (A) a high conductivity, high density material, reminiscent of a metal and (B) a low conductivity, low density material (an insulator). Material properties were: ρ_A=2500 kg/m^3, λ_A=100 W/m-K, Cp_A=1000 J/kg-K, α_A=4e-5 m^2/s; and ρ_B=2.5 kg/m^3, λ_B=0.1 W/m-K, Cp_B=1000 J/kg-K, α_B=4e-5 m^2/s. (Note that the thermal diffusivity, $\alpha=\lambda/(\rho Cp)$, for the two materials is exactly the same.)

For a uniform material, the temperature solution is given by Eq. (1):

$$T=T_1\left(1-\frac{x}{L}\right) \tag{1}$$

Note that the steady state solution (1) is independent of material properties, while a solution for the unsteady problem would be a function of the thermal diffusivity. When a mixture of the two materials is applied to the domain, the solution to this canonical test problem begins to vary. It is this mixture behavior and its dependence on scale that is of interest.

A. Steady State Conduction

Random mixtures of the two materials were constructed in which the relative volume fractions of A and B were exactly controlled to specified values. The domain is always fully filled so that the volume fractions f_A and f_B sum to unity. The proportions studied here ranged from f_A=0.0625, f_B=0.9375 to f_A=0.9375, f_B=0.0625 using steps of 0.0625 (1/16). The f_A=1, f_B=0 and f_A=0, f_B=1 cases are trivial and correspond with the analytical solution (1).

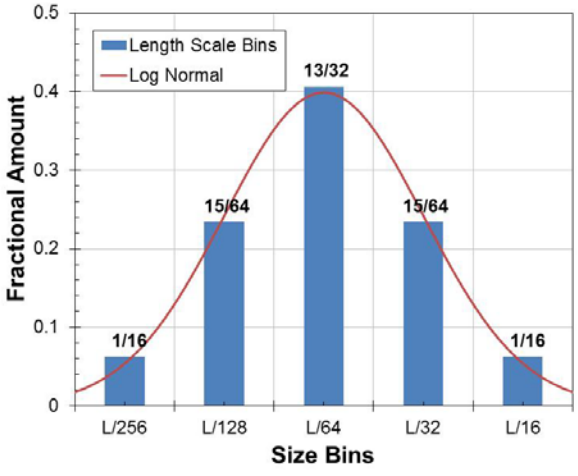

Fig. 1: Pseudo log normal distribution created by using mixture of size bins.

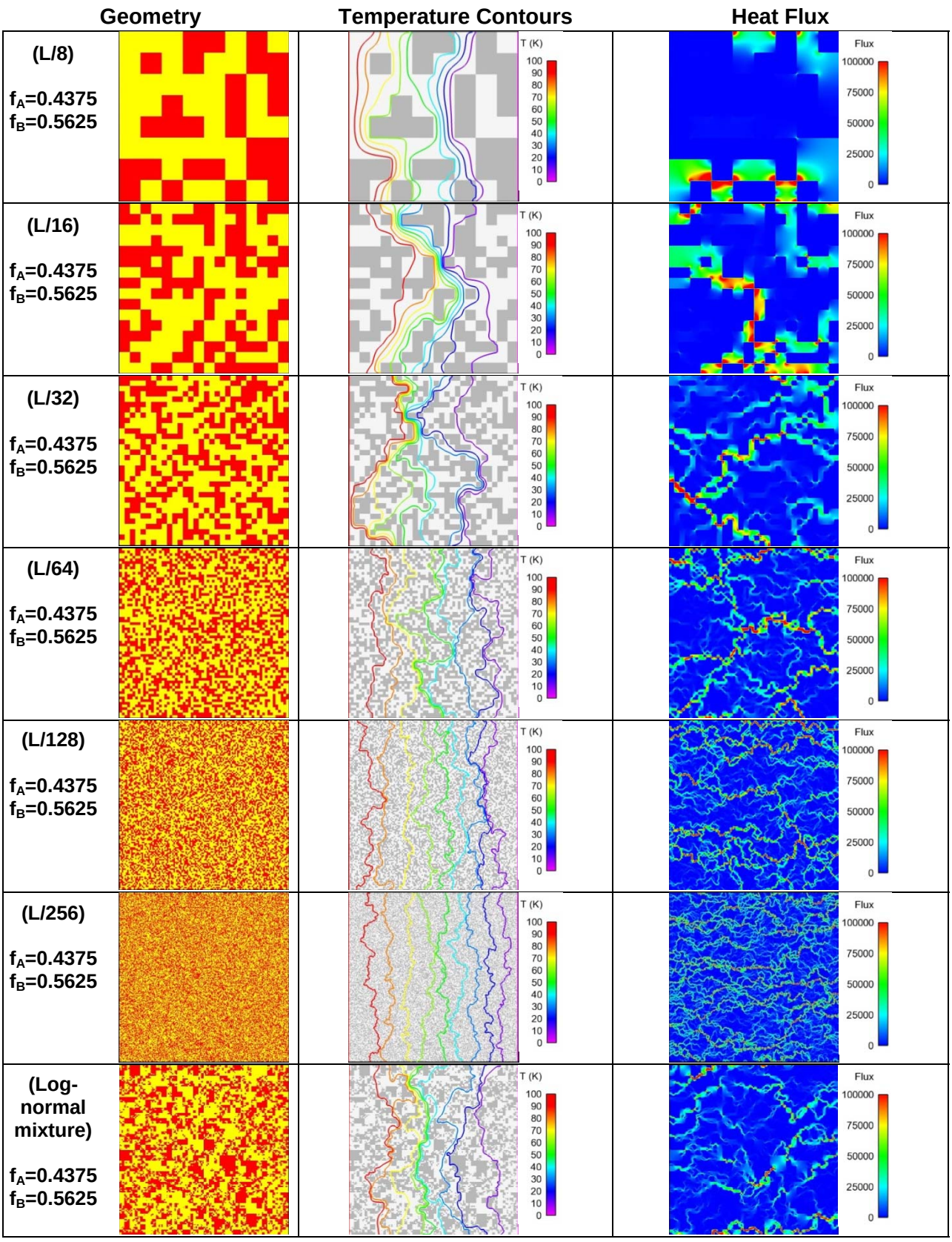

Fig. 2. Random mixtures at various length scales, isotherm contours, and heat fluxes.

Geometrical feature lengths were varied over six levels ranging from the coarsest with length scale of L/8 to the finest with length scale of L/256 where L is the overall domain length. For our test case of L=5.12 cm, the finest scale is 200 μm and the coarsest is 6.4 mm. Each of these geometries was considered monomodal; only features of the given size were included, whether that feature was of material A or of material B.

We also constructed some geometries with a "pseudo log normal" distribution. These consisted of mixtures of the various size scales such that proportions of each size bin approximately fits a Gaussian distribution with the abscissa represented on a log scale, as in Fig. 1. In this distribution, the fractions at the various scales were: L/16 =1/16, L/32 = 15/64, L/64 = 13/32, L/128 = 15/64, L/256 = 1/16. In the log normal distribution, the fractions of materials A and B were held constant over all length scale bins. That is for a f_A=0.25, f_B=0.75 case, one quarter of the L/16 size blocks were material A, one quarter of the size L/32 blocks were material A, and so forth.

The thermal transport was solved using the Sierra-Aria code developed and maintained at Sandia National Laboratories.[18] Extensive code and simulation verification has been performed on Aria for heat transfer simulations. Examples of the six different length scales (monomodal) and the log normal distribution are shown in Fig. 2 for f_A=0.4375, f_B=0.5625. Here the high conductivity material (A) is shown in red and the low conductivity (B) in yellow. The underlying finite element mesh for each of these cases is identical: a 512x512 element quad mesh. The corresponding temperature isotherm contours (with 10 K spacing) and heat flux pathways from steady state calculations are also shown.

Note that there are continuous heat flow pathways through the conductive portion of each of these instances shown. That is, a percolation network is established (though just barely for some cases such as the L/16 and L/32 instances shown in Fig. 2). However, it is clear from the figure that many of the pathways depend on heat transfer through shared corner nodes. This contrasts with a traditional two-dimensional site-bond lattice with four connections per site (north, south, east, and west). In that case we expect the percolation threshold to occur at a connection density of 0.5. It can be seen that in our geometry, percolation happens at a lower density (at least as low as f_A=0.4375 as seen in Fig. 2, other instances occur at even lower f_A values due to finite size effects). This is because of the shared corner node phenomenon which allows heat flow in diagonal directions (NE, NW, SE, and SW) in addition to the four ordinal directions.

Multiple randomized realizations were constructed at each geometrical scale. To characterize the variations, statistics were performed on the temperature at all 513 nodes at each x location (i.e. include all y values at a single value of x). Mean, standard deviation, and maximum and minimum values were computed. Typically one hundred different geometry realizations were combined at each scale level. Figure 3 shows an example of the temperature variations for one particular realization at a feature length scale of L/256 and f_A=f_B=0.5, with mean, maximum, and minimum on the left side graph and standard deviation on the right.

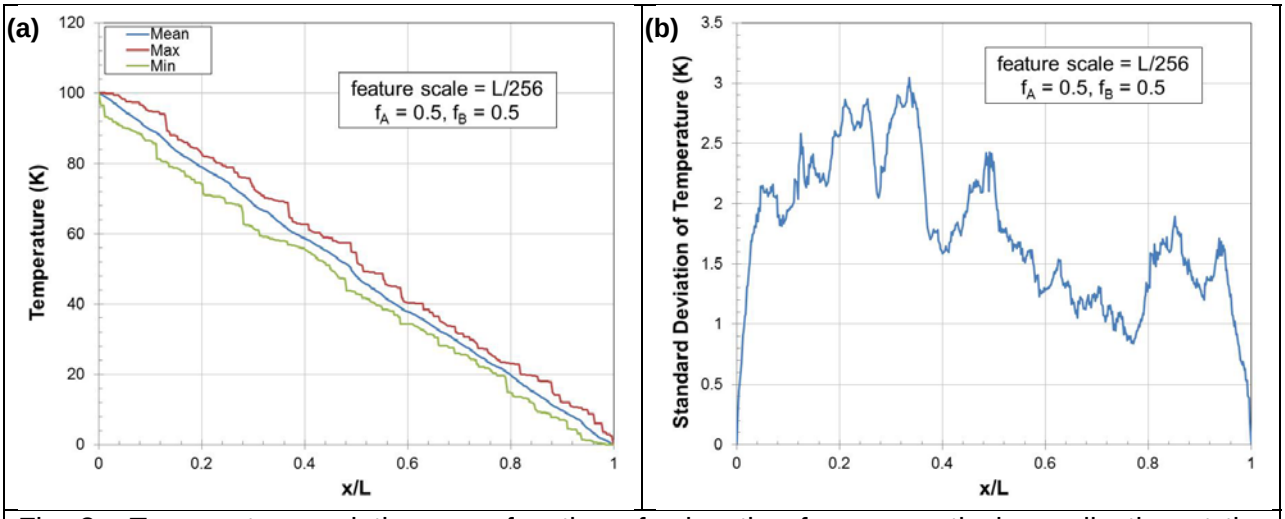

Fig. 3. Temperature variation as a function of x location for one particular realization at the feature scale of L/256 and f_A=f_B=0.5. (a) Mean, maximum, and minimum. (b) Standard deviation.

Figure 4 shows the compilation of one hundred realizations at the same length scale level (L/256) and volume fractions (f_A=f_B=0.5). Note that the jaggedness has been smoothed, and the mean line tracks the expected linear profile nicely, but there remains a certain level of variation, characterized by the maxima, minima and standard deviation. All three of these quantities exhibit "end effects;" the Dirichlet boundary conditions at x=0 and x=L limit the variations near these locations. Away from the ends, the level of variation (both in max/min range and in standard deviation) approach constant values. We have chosen standard deviation and maximum-to-minimum range as metrics for comparing between different length scales and volume fractions. For each set of conditions (usually consisting of 100 realizations), standard deviation and max-to-min range data between x/L of 0.25 and 0.75 were averaged to remove end effects. Figure 5 shows these variations. Note that there is a strong amplification of the variation as the percolation threshold (at f_A~0.4) is approached from either side.

In addition to the temperature variations, another characteristic that can be assessed is the so-called effective thermal conductivity of the mixture. This is done by computing the total integrated flux leaving the system at x=L, then dividing by the area and overall thermal gradient. Fig. 6 shows the effective thermal conductivity as a function of the fraction of the two components for the various different feature sizes (L/8 to L/256).

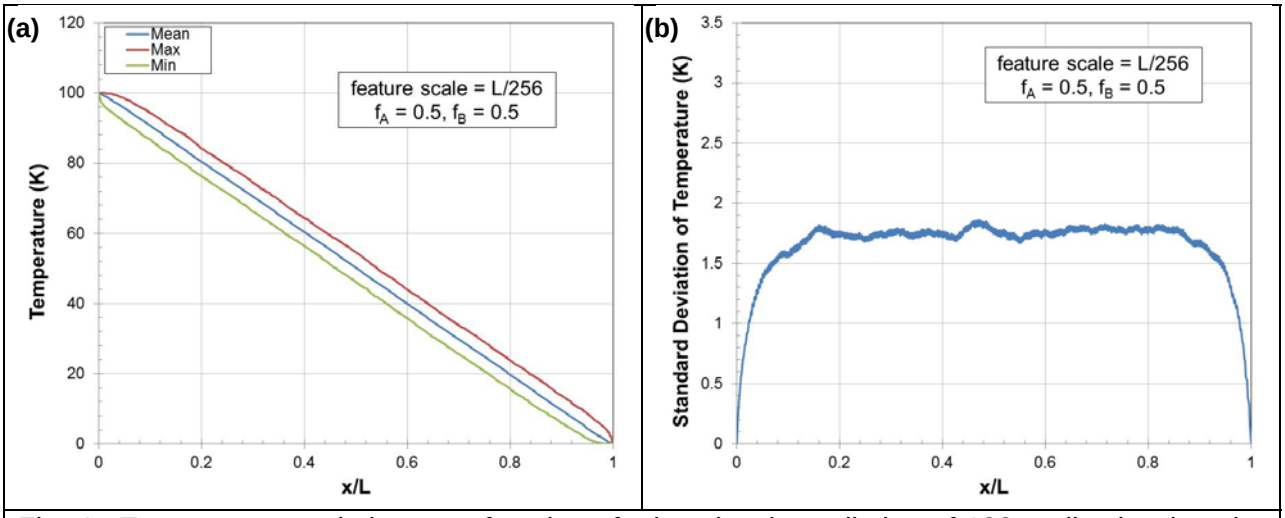

Fig. 4. Temperature variation as a function of x location (compilation of 100 realizations) at the feature scale of L/256 and f_A=f_B=0.5. (a) Mean, maximum, and minimum. (b) Standard deviation.

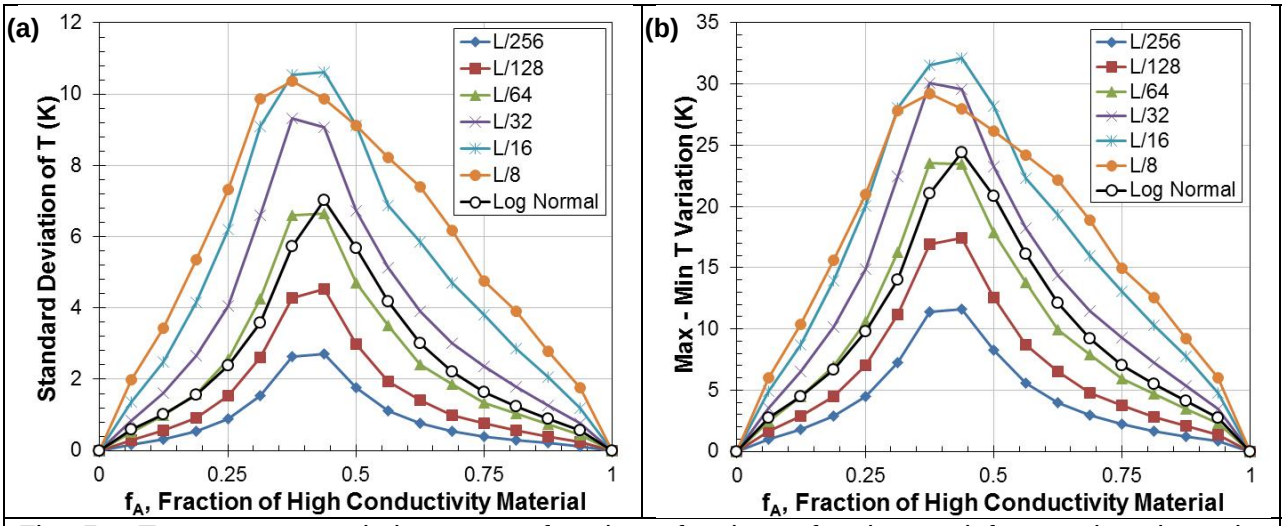

Fig. 5. Temperature variations as a function of volume fraction and feature length scale. (a) standard deviation. (b) Maximum-to-minimum range.

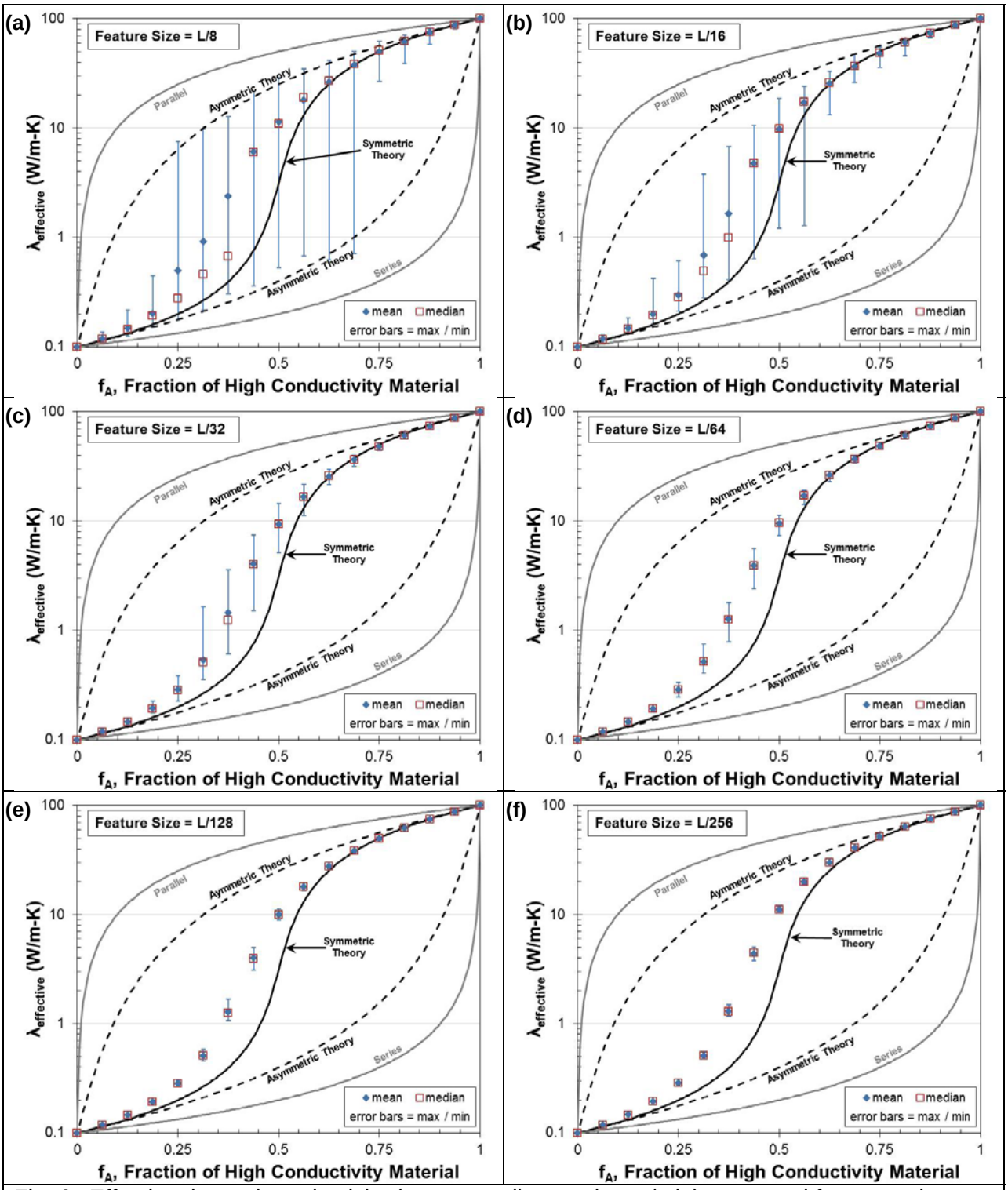

Fig. 6. Effective thermal conductivity (mean, median, and max/min) computed from steady-state simulations. At least 100 geometric realizations were used in computing each of the points on these graphs. Also shown are symmetric and asymmetric effective media theory lines and parallel and series limiting cases. Feature length scales were: (a) L/8, (b) L/16, (c) L/32, (d) L/64, (e) L/128, (f) L/256.

All of the results in Fig. 6 were based on statistics of at least 100 geometric realizations at each f_A and feature length scale. Mean, median, and maximum/minimum are shown. A logarithmic scale is used for the ordinate to illustrate the full range of behavior. Also shown are some theoretical results, including the symmetric (Eq. 2) and asymmetric (Eq. 3a, b) effective medium theories (i.e. Bruggeman theory) and the parallel and series upper and lower limits. The effective medium theory expressions are given here, where λ_{mix} is the mixture thermal conductivity and d is the dimensionality of the geometry (d=2 in our example). Also given are the parallel (Eq. 4) and series (Eq. 5) forms of the mixture rules.

Symmetric
$$f_A \frac{(\lambda_A-\lambda_{mix})}{(\lambda_A+(d\text{-}1)\lambda_{mix})} + f_B \frac{(\lambda_B-\lambda_{mix})}{(\lambda_B+(d\text{-}1)\lambda_{mix})} = 0 \quad (2)$$

Asymmetric
$$\frac{(\lambda_{mix}-\lambda_A)^d}{\lambda_{mix}} = \frac{(1-f_A)^d(\lambda_B-\lambda_A)^d}{\lambda_B} \quad (3a)$$

Asymmetric
$$\frac{(\lambda_{mix}-\lambda_B)^d}{\lambda_{mix}} = \frac{(1-f_B)^d(\lambda_A-\lambda_B)^d}{\lambda_A} \quad (3b)$$

Parallel
$$\lambda_{mix} = f_A\lambda_A + f_B\lambda_B \quad (4)$$

Series
$$\lambda_{mix} = \frac{1}{f_A/\lambda_A+f_B/\lambda_B} \quad (5)$$

There are a few interesting points to be brought out. First, as expected, all the results are indeed bounded by the parallel and series limits. Next, we see clear indications of higher variability (the difference between mean and median values along with the large max-to-min ranges) with the coarser length scale models, as compared with the finer length scale models. Again, this is not surprising. The largest changes and variations in effective thermal conductivity occur near the percolation threshold, circa f_A=0.4.

It is also interesting to compare these results with the Bruggeman effective medium theories (symmetric and asymmetric). Note that the simulations show a similar shape to the symmetric theory line but are noticeably offset. The symmetric theory line indicates a percolation threshold right at f_A=0.5; here we observe the transition at a somewhat lower f_A value. It is also interesting to note that the max-to-min range variations at the coarsest (L/8) simulated scale nearly correspond with the Bruggeman asymmetric formulas. The asymmetric formulas are meant to describe the situations where one has inclusions of material B in a continuous matrix of material A or vice versa.

Given that the variability, and therefore uncertainty, decreases as the size of the microstructure becomes small compared to the domain length, a first approach to reduce aleatoric uncertainty for thermal transport in heterogeneous media appears to be to increase the domain length. However, reducing uncertainty for a heterogeneous media across all scales in this fashion will not be viable in cases when the microstructural scale is set by some fundamental feature size. In our results, the minimum to maximum variation in temperature was still 10K for the finest structure computed, L/256, near the percolation threshold so variability and associated uncertainty is inherent for heterogeneous materials. When the limits of reducing aleatoric uncertainty by increasing the domain size have been reached, sufficient simulations are required to capture the variations in the material through statistical means such as generating the probability density function.[8,14] These probability density functions are then a mechanism by which the uncertainties can be propagated between scales in a multiscale thermal transport simulation.[7,16-17]

Although we principally consider UQ behavior, the simulations performed here in some respects also address model validation. To this end, we can state that as bounding conditions, the parallel and series "models" are validated—every simulation case falls between them. In contrast, the small but noticeable difference between the symmetric effective medium theory (the "model") and our simulation results (numerical "experiments") points to a model which is not validated; there are aspects of the simulations (likely the shared corner phenomenon) which are not captured by the effective medium theory model. There is evidently a difference in the "physics" represented by the symmetric model and our simulations. Note that we do not state which of these most closely represents reality (an actual geometry constructed of actual material); from this perspective it is better to speak of verification of the simulations in appropriate limits corresponding to the theoretical assumptions of the effective medium approximation.

IV. Conclusions

The increasing use of multiscale transport models necessitates the development of uncertainty quantification methodologies applicable to multiscale heat transfer simulations. Heterogeneous mixtures can exhibit microstructure on a scale not much smaller than the computational domain which impacts the predicted material variability and calculated aleatoric uncertainty. The aleatoric uncertainty is that due to inherent randomness and is illustrated for steady state thermal transport in a two component mixture. The ratio of the domain length, L, to the microstructure size was varied from L/8 to L/256 and the volume fraction of high conductivity material, f_A, varied from 0 to 1. A peak in the uncertainty, variability, was observed near the percolation threshold of around f_A of 0.4 and decreased by a factor of 2 from the peak for f_A's greater than 0.75 or less than 0.25. The uncertainties in the temperatures, as captured by the maximum – minimum values for the simulations, were around 30K for the coarser structures: L/8, L/16, and L/32; and as much as 10K for the finest structure: L/256. The range of the effective thermal conductivities varied by over an order of magnitude for the coarser L/8 and L/16 microstructures. Statistical representations of the aleatoric uncertainty for heterogeneous materials are necessary and need to be passed between scales in multiscale simulations of thermal transport.

Acknowledgments

Sandia National Laboratories is a multi-program laboratory managed and operated by Sandia Corporation, a wholly owned subsidiary of Lockheed Martin Corporation, for the U.S. Department of Energy's National Nuclear Security Administration under contract DE-AC04-94AL85000.

References

[1]Murthy, J. Y., and Mathur, S. R., "Computational Heat Transfer in Complex Systems: A Review of Needs and Opportunities," *ASME Journal of Heat Transfer*, Vol. 134, Paper No. 031016, 2012, 12 pp.

[2]DeVolder, B., Glimm, J., Grove, J. W., Kang, Y., Lee, Y., Pao, K., Sharp, D. H., and Ye, K., "Uncertainty Quantification for Multiscale Simulations," *ASME Journal of Fluids Engineering*, Vol. 124, 2002, pp. 29-41.

[3]He, Y.-L., and Tao, W.-Q., "Multiscale Simulations of Heat Transfer and Fluid Flow Problems," *ASME Journal of Heat Transfer*, Vol. 134, Paper No. 031018, 2012, 13 pp.

[4]Pilch, M., Trucano, T. G., and Helton, J. C., "Ideas Underlying the Quantification of Margins and Uncertainties," *Reliability Engineering and System Safety*, Vol. 96, 2011, pp. 965-975.

[5]Roy, C. J., and Oberkampf, W. L., "A Comprehensive Framework for Verification, Validation, and Uncertainty Quantification in Scientific Computing," *Computer Methods in Applied Mechanics and Engineering*, Vol. 200, 2011, pp. 2131-2144.

[6]ASME V&V 20 Committee, "Standard for Verification and Validation in Computational Fluid Dynamics and Heat Transfer," ASME V&V 20-2009, November 30, 2009.

[7]Marepalli, P., Qiu, B., Ruan, X., and Murthy, J. Y., "Quantifying Uncertainty in Multiscale Heat Conduction Calculations," *Proceedings of the ASME 2012 Summer Heat Transfer Conference*, HTC2012-58523, 2012, 10 pp.

[8]Lechman, J. B., Yarrington, C., Erikson, W., and Noble, D. R., "Thermal Conduction in Particle Packs via Finite Elements," *Powders and Grains 2013, AIP Conf. Proc.*, Vol. 1542, 2013, pp. 539-542.

[9]Ganapathysubramanian, B., and Zabaras, N., "Modeling Multiscale Diffusion Processes in Random Heterogeneous Media," *Computer Methods in Applied Mechanics and Engineering*, Vol. 197, 2008, pp. 3560-3573.

[10]Jiang, F., and Sousa, C. M., "Effective Thermal Conductivity of Heterogeneous Multi-Component Materials: an SPH Implementation," *Heat and Mass Transfer*, Vol. 43, 2007, pp. 479-491.

[11]Wang, J., Carson, J. K., North, M. F., and Cleland, D. J., "A New Approach to Modelling the Effective Thermal Conductivity of Heterogeneous Materials," *International Journal of Heat and Mass Transfer*, Vol. 49, 2006, pp. 3075-3083.

[12]Miettinen, L., Kekäläinen, P., Turpeinen, T., Hyväluoma, J., Merikoski, J., and Timonen, J., "Dependence of Thermal Conductivity on Structural Parameters in Porous Samples," *AIP Advances*, Vol. 2, Paper No. 012101, 2012, 15 pp.

[13]Gusarov, A. V., and Kovalev, E. P., "Model of Thermal Conductivity in Powder Beds," *Physical Review B*, Vol. 80, Paper No. 024202, 2009, 15 pp.

[14]Ostoja-Starzewski, M., "Random Field Models of Heterogeneous Materials," *International Journal of Solids and Structures*, Vol. 35, No. 19, 1998, pp. 2429-2455.

[15]Chernatynskiy, A., Phillpot, S. R., and LeSar, R., "Uncertainty Quantification in Multiscale Simulation of Materials: A Perspective," *Annual Review of Materials Research*, Vol. 43, 2013, pp. 157-182.

[16]Koslowski, M., and Strachan, A., "Uncertainty Propagation in a Multiscale Model of Nanocrystalline Plasticity," *Reliability Engineering and System Safety*, Vol. 96, 2011, pp. 1161-1170.

[17]Fish, J., "Bridging the Scales in Nano Engineering and Science," *Journal of Nanoparticle Research*, Vol. 8, 2006, pp. 577-594.

[18]Notz, P. K., Subia, S. R., Hopkins, M. W., Moffat, H. K., and Noble, D. R., "Aria 1.5: User Manual," SAND2007-2734, Sandia National Laboratories, Albuquerque, New Mexico, 2007.